

Protonation of the Dinitrogen-Reduction Catalyst [HIPTN₃N]Mo^{III} Investigated by ENDOR Spectroscopy

R. Adam Kinney,[†] Rebecca L. McNaughton,[†] Jia Min Chin,[‡] Richard R. Schrock,^{*,‡} and Brian M. Hoffman^{*,†}

[†]Department of Chemistry, Northwestern University, Evanston, Illinois 60208, United States, and

[‡]Department of Chemistry, Massachusetts Institute of Technology, Cambridge, Massachusetts 02139, United States

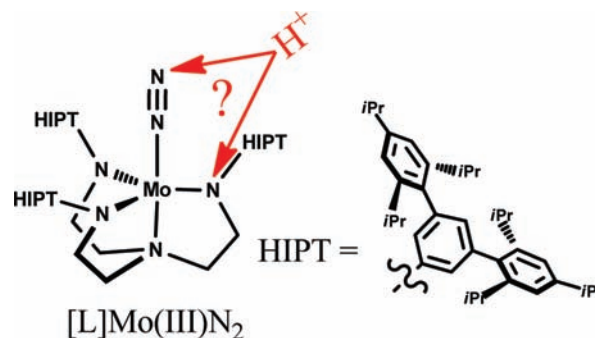
Received October 21, 2010

Dinitrogen is reduced to ammonia by the molybdenum complex of L = [HIPTN₃N]³⁻ [Mo; HIPT = 3,5-(2,4,6-*i*-Pr₃C₆H₂)₂C₆H₃]. The mechanism by which this occurs involves the stepwise addition of proton/electron pairs, but how the first pair converts MoN₂ to MoN=NH remains uncertain. The first proton of reduction might bind either at N_β of N₂ or at one of the three amido nitrogen (N_{am}) ligands. Treatment of MoCO with [2,4,6-Me₃C₆H₃]BAR'₄ [Ar' = 2,3-(CF₃)₂C₆H₃] in the absence of reductant generates HMoCO⁺, whose electron paramagnetic resonance spectrum has greatly reduced *g* anisotropy relative to MoCO. ²H Mims pulsed electron nuclear double-resonance spectroscopy of ²HMoCO⁺ shows a signal that simulations show to have a hyperfine tensor with an isotropic coupling, *a*_{iso}(²H) = -0.22 MHz, and a roughly dipolar anisotropic interaction, *T*(²H) = [-0.48, -0.93, 1.42] MHz. The simulations show that the deuteron is bound to N_{am}, near the Mo equatorial plane, not along the normal, and at a distance of 2.6 Å from Mo, which is nearly identical with the (N_{am})²H⁺-Mo distance predicted by density functional theory computations.

Molybdenum complexes of the L = [HIPTN₃N]³⁻ ligand [HIPT = 3,5-(2,4,6-*i*-Pr₃C₆H₂)₂C₆H₃] catalytically reduce dinitrogen to ammonia under mild conditions.¹ The mechanism proposed for this process, a stepwise addition of proton/electron pairs, rests on the intermediate states that have been isolated and characterized to date. However, the mechanism by which the first proton/electron pair converts MoN₂ (Mo = [L]Mo) into MoN=NH (MoNNH) is unknown. This transformation occurs rapidly in the presence of a reductant, CoCp₂ or CrCp*₂, and any one of the acids [Et₃NH][OTf], [Et₃NH][BAR'₄], or [2,6-LutH][BAR'₄]. Three mechanistic routes have been considered: (i) reduction followed by protonation, either at N_β on the dinitrogen ligand or an amido N (N_{am}) of [L]; (ii) protonation of either type of nitrogen, followed by reduction; or (iii) proton-coupled electron transfer, again with alternate sites for the proton. To achieve a comprehensive understanding of the reduction mechanism, it

is of importance to identify the site at which a proton is most likely to interact (Scheme 1).

Scheme 1



In the absence of a reducing agent, the addition of 1 equiv of LutH⁺ to MoN₂ [$\nu(\text{NN}) = 1990 \text{ cm}^{-1}$] generates a new species, HMoN₂⁺, with a $\nu(\text{NN})$ stretch increased to 2057 cm^{-1} . This shift is consistent with decreased back-bonding to the dinitrogen ligand; however, no new low-energy band is observed, as would be expected if N_β of the dinitrogen ligand were protonated. Similarly, when MoCO [$\nu(\text{CO}) = 1885 \text{ cm}^{-1}$] is treated with 1 equiv of LutH⁺, a new species, HMoCO⁺, appears with $\nu(\text{CO})$ increased to 1932 cm^{-1} ,² again because of diminished back-bonding.³ Unfortunately, although the amount of protonated MoN₂ increases with the amount of LutH⁺ added, attempts to measure an equilibrium between MoN₂ and HMoN₂⁺ failed because the complexes undergo concomitant decomposition,³ most plausibly because the loss of protonated [L] is facile.

As an alternative approach to investigating the site at which a proton interacts with MoAB (AB = CO, N₂), we have applied electron paramagnetic resonance (EPR) and ²H electron nuclear double-resonance (ENDOR) spectroscopy to samples of these MoAB treated with LutD⁺ in the absence of a reducing agent.

*To whom correspondence should be addressed. E-mail: rrs@mit.edu (R.R.S.), bmh@northwestern.edu (B.M.H.).

(1) Yandulov, D. V.; Schrock, R. R. *Science (Washington, DC)* 2003, 301, 76–78.

(2) We have been unable to identify any features in the IR spectrum of MoAB, AB = CO, or N₂ treated with LutH⁺ that are consistent with a new NH stretch.

(3) Schrock, R. R. *Angew. Chem., Int. Ed.* 2008, 47, 5512–5522.

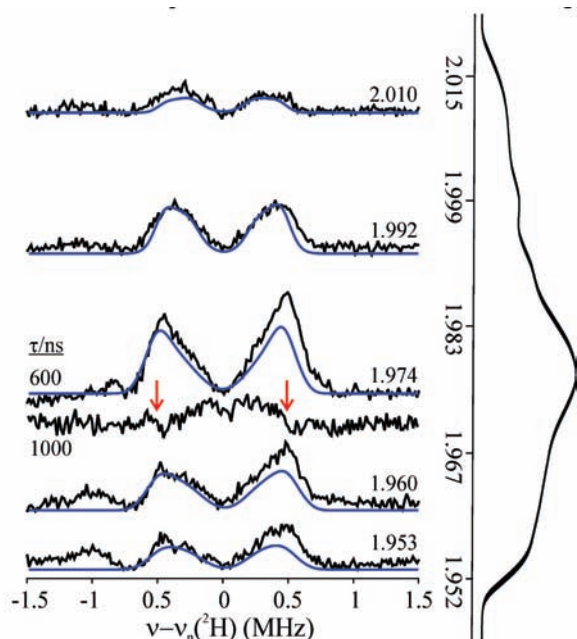


Figure 1. 35 GHz Mims ^2H ENDOR field-frequency pattern for $^2\text{HMoCO}^+$: $A = [-0.70, -1.15, 1.2]$ MHz; orientation relative to g , $(\alpha, \beta, \gamma) = (25, 65, 0)$. Hyperfine suppression holes are indicated with red arrows for the $\tau = 1 \mu\text{s}$ spectrum taken at $g = 1.974$. The EIE spectrum was generated by plotting the intensity of the ν_+ ^2H ENDOR response versus field and then applying a spline fit to the data.

Treatment⁴ of $S = 1/2$ MoCO with LuH/D^+ leads to a new signal in the echo-detected EPR spectrum with a small g spread, $\mathbf{g} = [2.010, 1.974, 1.953]$ (Figures 1 and S1 in the Supporting Information), in contrast with that of MoCO , whose g values are strongly shifted from the free-electron value, $g_{\parallel} = 3.1$ and $g_{\perp} = 1.6$, and determined by the Jahn–Teller (JT) effect.⁵ Only a small percentage of MoCO is converted, consistent with the prior results noted above.

We applied pulsed ENDOR spectroscopy⁶ to the new species formed by treatment of MoCO with LuD^+ to directly determine the presence and location of a bound deuteron. Mims ENDOR spectra⁷ taken at multiple fields across the new EPR signal display a doublet pattern centered at the ^2H Larmor frequency, with a hyperfine splitting of approximately $A(^2\text{H}) \sim 1$ MHz (Figure 1), corresponding to $A(^1\text{H}) = 6.5$ MHz. The assignment of this signal as a ^2H ENDOR response is confirmed by its suppression in a spectrum taken with the spacing between the first and second pulses of the Mims sequence of $\tau = 1 \mu\text{s}$. The Mims ENDOR intensity is modulated by the response factor $R \sim [1 - \cos(2\pi A\tau)]$. For an $A = 1$ MHz coupled deuteron, the Mims ENDOR response should be suppressed when $\tau = 1 \mu\text{s}$, as observed in the spectrum collected at $g = 1.974$ (Figures 1 and S2 in the Supporting Information).

To confirm that the ^2H ENDOR response is associated with $^2\text{HMoCO}^+$ and does not arise from the background

(4) A 5 mM solution of MoCO in toluene was treated with 1 equiv of $[2,4,6\text{-Me}_3\text{C}_5\text{H}_3\text{N}]\text{BAR}^4$ at room temperature and stirred. Solutions of protonated MoN_2 were generated likewise.

(5) McNaughton, R. L.; Roemelt, M.; Chin, J. M.; Schrock, R. R.; Neese, F.; Hoffman, B. M. *J. Am. Chem. Soc.* **2010**, *132*, 8645–8656.

(6) Davoust, C. E.; Doan, P. E.; Hoffman, B. M. *J. Magn. Reson.* **1996**, *119*, 38–44.

(7) Schweiger, A.; Jeschke, G. *Principles of Pulse Electron Paramagnetic Resonance*; Oxford University Press: Oxford, U.K., 2001.

EPR signal of MoCO , we collected the ENDOR-induced EPR (EIE) spectrum associated with the ^2H signal.⁷ A 2D field-frequency pattern of ^2H ENDOR spectra was collected at multiple points across the range of fields that yield a ^2H ENDOR response. The ^2H ENDOR signal does not extend past the narrow range of fields assigned to the $^2\text{HMoCO}^+$ EPR signal. A fit of the ν_+ peak intensities from the 2D pattern of ENDOR spectra to a spline curve yielded the EIE spectrum of $^2\text{HMoCO}^+$ presented in Figure 1, with g values corresponding to those given above.

The 2D field-frequency ^2H ENDOR pattern of Figure 1 was simulated⁸ to determine the hyperfine tensor of the bound deuteron and, through this, to obtain insight into its location and chemical environment. The pattern is well simulated by a hyperfine tensor having components $A(^2\text{H}) = [-0.70(10), -1.15(05), 1.2(1)]$ MHz, which is oriented relative to g by the Euler angles $(\alpha, \beta, \gamma) = (25, 65, 0)$.⁹ This interaction corresponds to an isotropic coupling, $a_{\text{iso}}(^2\text{H}) = -0.22$ MHz, and a roughly dipolar anisotropic interaction, $T(^2\text{H}) = [-0.48, -0.93, 1.42]$ MHz.¹⁰ To test the assignment of the species being studied as $\text{Mo-N}_{\text{am}}(^2\text{H}^+)$, we performed a density functional theory (DFT) optimization on an N_{am} -protonated MoCO (Figure 2 and Table 1).¹¹ The low g aniso-

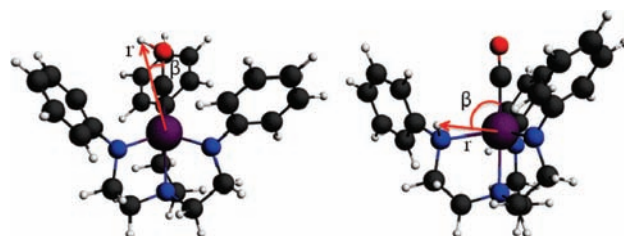


Figure 2. DFT-optimized structures for CO-protonated (left) and N_{am} -protonated (right) MoCO . The predicted values of r and β are 3.65 Å and 13°, respectively, for the CO proton and 2.7 Å and 88°, respectively, for the N_{am} proton (g_1 is expected to be nearly coincident with the Mo-C bond axis).

tropy of the new spectrum indicates a strong reduction from the 3-fold symmetry of the parent MoCO . The DFT geometry optimization of the N_{am} -protonated HMoCO^+ is consistent with such a symmetry reduction; the length of the $\text{Mo-N}_{\text{am}}(\text{H}^+)$ bond is predicted to be approximately 13% longer than the Mo-N_{am} bond. This reduction from 3-fold symmetry at Mo readily accounts for the suppression of JT effects implied by the small g anisotropy. If, instead, the oxygen of the axial CO

(8) Doan, P. E. The Past, Present, and Future of Orientation-Selected ENDOR Analysis: Solving the Challenges of Dipolar-Coupled Nuclei. In *Paramagnetic Resonance of Metallobiomolecules*; Telser, J., Ed.; American Chemical Society: Washington, DC, 2003; pp 55–81.

(9) The quadrupole splitting for the deuteron is not resolved in the ENDOR spectra, but its incorporation into the simulations is necessary to obtain quality fits. From the simulations, we predict principal values of $P = [-0.075, 0.034, 0.039]$ MHz, with an orientation relative to that of g of $(\alpha, \beta, \gamma) = (0, 55, 0)$.

(10) The isotropic and dipolar hyperfine couplings are calculated from the expression $A = a_{\text{iso}} + T$. Absolute signs for the principal hyperfine values were not directly determined. Rather, the sign of a_{iso} must be negative because the maximum dipolar component is positive, $T_3 > 0$.

(11) DFT calculations were performed with the Amsterdam Density Functional (ADF) software package (ADF version 2007.01, SCM, Theoretical Chemistry, Vrije Universiteit, Amsterdam, The Netherlands, <http://www.scm.com>) with a BLYP functional in the spin-unrestricted formalism. Geometry optimizations used a TZ2P basis set with a small core potential for all atoms. A reduced structure for Mo, in which the HIPT groups were replaced with phenyls, was used for geometry optimization.

Table 1. Selected DFT-Optimized Bond Lengths^a and Angles for MoCO Protonated Either at an Amido Nitrogen or the Carbonyl Oxygen

	MoH ⁺		MoN _{am}		MoN _{ax}	MoC	CMoH ⁺	N _{am} MoN _{am}		N _{ax} MoC	
N _{am} -H ⁺	2.690	2.302	2.006	1.977	2.315	2.017	88.2	118.2	110.9	120.8	177.3
CO-H ⁺	3.647	2.057	2.055	2.053	2.348	1.189	13.1	117.7	115.3	116.5	179.3

^a See ref 4 for computational details.

were protonated, DFT computations (Figure 2 and Table 1) indicate that the resultant species very nearly retains the trigonal symmetry of the parent. Such a complex would exhibit large *g* anisotropy, like that of MoCO, contrary to observation.

The observed hyperfine tensor also is consistent with N_{am} protonation. Taking the experimental $T_3 = 1.42$ MHz as an effective through-space dipolar coupling constant, $T_3 = 2T = 2g_e\beta_e g_n\beta_n/r^3$, gives $r = 2.6$ Å, consistent with that predicted for a point-dipole interaction between the Mo spin and N⁻²H⁺ at the distance calculated from the DFT geometry optimization (2.7 Å, Table 1), $2T = 1.26$ MHz.¹² In contrast, for protonation at the carbonyl oxygen, the DFT geometry gives $r \sim 3.65$ Å, with $2T \sim 0.50$ MHz, much smaller than that observed. More importantly perhaps, the Mo⁻²H⁺ vector for CO protonation would lie roughly along the *g*₁ direction, $\beta \sim 13^\circ$, whereas the Mo⁻²H vector for N_{am} protonation lies at $\beta = 88^\circ$, in acceptable agreement with the simulations, $\beta = 65^\circ$. In short, both the *g* tensor and the ²H hyperfine tensor are in agreement with N_{am} protonation and not with CO protonation. An equivalent argument rules out protonation of the “distal” axial nitrogen of [L].

The properties of the ²H hyperfine tensor for N_{am}(²H⁺) of the LuH⁺-treated MoCO complex provide support for our recent assignment of the species trapped in frozen solutions when MoN₂ is treated with H₂ gas. This species was assigned as the hydridomolybdenum(III) anion formed by heterolytic cleavage of H₂ and loss of H⁺. If, instead, this species were the neutral complex formed by heterolytic H₂ cleavage, with the proton bound as N_{am}(H⁺) and the hydride bound to Mo^{III}, it would necessarily show an ENDOR signal equivalent to that seen here from N_{am}(²H⁺), but it does not.

We were unsuccessful in trapping the analogous protonated MoN₂ at low temperature in an EPR tube, with the complex instead presumably decomposing to unidentified species through loss of the protonated organic ligand.

(12) Snetsinger, P. A.; Chasteen, N. D.; van Willigen, H. *J. Am. Chem. Soc.* **1990**, *112*, 8155–8160.

(13) Kinney, R. A.; Hettterscheid, D. G. H.; Hanna, B. S.; Schrock, R. R.; Hoffman, B. M. *Inorg. Chem.* **2010**, *49*, 704–713.

Following our earlier discussion of the modes of decomposition of the product(s) of the reaction of H₂ with Mo,¹³ it seems likely that protonation of MoN₂, like protonation of MoCO, occurs at the amido nitrogen and that the bond between Mo and N_{am}(H⁺) of amido-protonated MoN₂ cleaves to form an “arm-off” species that is unstable to total ligand loss, possibly through bimolecular processes. An alternative is that dinitrogen is lost from the cationic species more readily than CO is lost, again with an overall decomposition. The same type of frequency change to the N–N and C–O stretches upon treatment of the respective parent species with LuH⁺ suggests that protonation occurs at the same site in both systems.

In summary, a combination of EPR/ENDOR spectroscopy and DFT computations shows that treatment of MoCO with the acid LuH⁺ results in protonation of the amido nitrogen of the HIPTN₃N³⁻ ligand. IR spectroscopic measurements show that MoCO and MoN₂ behave similarly when treated with LuH⁺ in the absence of reductant, which strongly suggests that N_{am} is protonated in the same way, although protonated MoN₂ is too unstable to be trapped for EPR/ENDOR analysis. That N_{am} is the site of protonation for MoAB, AB = CO and N₂, further indicates that when acid and reductant are both present, then reduction of MoN₂ proceeds either by protonation of N_{am}, followed by electron transfer, or by proton-coupled electron transfer. This finding also provides evidence for N_{am} protonation as the first step in the acid-induced decomposition of [HIPTN₃N]Mo^{III}N₂.

Acknowledgment. This work was supported by the NIH (Grant HL13531 to B.M.H., Grant GM31978 to R.R.S., and Grant GM067349 to R.L.M.).

Supporting Information Available: Echo-detected EPR spectra, effect of varying τ on the Mims ²H ENDOR response, and complete 2D field-frequency pattern of Mims ENDOR spectra. This material is available free of charge via the Internet at <http://pubs.acs.org>.